Vision through semireflecting media: polarization analysis

Yoav Y. Schechner and Joseph Shamir

Department of Electrical Engineering, Technion—Israel Institute of Technology, Haifa, 32000, Israel

Nahum Kiryati

Department of Electrical Engineering—Systems, Faculty of Engineering, Tel Aviv University, Ramat Aviv, 69978, Israel

Received April 19, 1999

We present an approach to recovering scenes deteriorated by reflections off a semi-reflecting medium. The approach is based on imaging through a polarizer at two different orientations. We analyze the image-formation process, taking into account changes in reflection and polarization properties owing to internal reflections within the medium. Reconstruction by inverting this process requires estimation of the incidence angle (the inclination of the transparent medium). We estimate this angle by seeking the value that leads to decorrelation of the estimated scenes that are automatically and uniquely labeled reflected–transmitted.

OCIS codes: 100.2960, 100.3020, 260.5430, 150.0150.

The situation in which more than one (typically two) linearly superimposed images exist is often encountered in real-world scenes. For example,[1–3] looking out a car (or room) window, we see both the outside world, termed a real object,[2,4] and a semireflection of the objects inside, termed virtual objects. The separation of unrelated contributions to a scene is important for understanding and analysis of the scene. In fact, the mere detection of such a superposition indicates the presence of a clear (invisible) surface at a distance closer than the actual imaged objects.[2,4] Earlier approaches to reconstructing each of the contributions relied mainly on triangulation[5] and on focus.[2] These methods have several drawbacks, such as ill-conditioned reconstruction at low spatial frequencies, and they cannot determine which of the reconstructed images is of the real object and which is of the virtual one. The use of polarization in scene analysis has gained interest in recent years, particularly for analyzing reflections off opaque media, as in Ref. 6. As for removal of the virtual scene reflected by transparent media, other researchers attempted to do this by using just the raw output of a polarization analyzer,[1,3,4] but this technique works well only at the Brewster angle. While revising this Letter we were informed of some research conducted in parallel to ours[7] in which independent component analysis of polarization-filtered images was used. That research demonstrates the potential of polarization filtering as an initial step for separation by signal postprocessing; however, it still cannot determine which of the images corresponds to the real object, and the intensity is evaluated up to an unknown factor. Previous methods did not extract information about the invisible semireflecting surface itself.

Here we present an analysis of the physical process and demonstrate an approach to the reconstruction of the intensities of the contributing scenes. The reconstructed scenes are automatically labeled virtual or real, and the angle of incidence (AOI) on the transparent surface is estimated as well.

Assuming illumination by natural light, we represent the intensity by its polarization components parallel ($\|$) and perpendicular ($\perp$) to the plane of incidence with their respective reflectivities[8] $R_\|$ and $R_\perp$ and transmissivities $T_\|$ and $T_\perp$ at each interface. In most cases, such as observation through a window, two surfaces are involved, and internal reflections must be considered. It is easy to show that, for lossless media and incoherent light, the total reflectivity of a double-surfaced window is given by the relation

$$\tilde{R} = R + T^2 R \sum_{l=0}^{\infty} (R^2)^l = \frac{2}{1+R} R \qquad (1)$$

for each polarization component. By energy conservation, the total transmissivities are $\tilde{T} = 1 - \tilde{R}$ for each component.

To derive the physical principles of the proposed procedure we may define polarizing effects (PE's) of reflection and transmission by the degree of polarization induced on unpolarized light; for reflection from a window it is $\mathrm{PE}_R \equiv |\tilde{R}_\perp - \tilde{R}_\||/|\tilde{R}_\perp + \tilde{R}_\||$. Theoretically, the PE's can be derived from the Fresnel equations[8] as a function of AOI. For example, for a single-surface medium, $\mathrm{PE}_R = 1$ at the Brewster angle, at which the parallel component vanishes, and it is zero for AOI $\varphi = 0°, 90°$. For transmission, $\mathrm{PE}_T \equiv |\tilde{T}_\perp - \tilde{T}_\||/|\tilde{T}_\perp + \tilde{T}_\||$. For a double-surfaced window, at most incidence angles φ, PE_T is almost double that of a single surface and amounts to ~10% (and even more) of PE_R (Fig. 1). Therefore one cannot assume that the polarization of the transmitted light is negligible relative to the polarization of the reflected light. Hence for the separation of the scenes one cannot generally assume that solely the virtual scene is associated with partial polarization.

We denote the spatial intensity distribution that is due to the real scene (with no window) by I_T and the spatial distribution that is due to the virtual scene (assuming perfect mirror replacing the window) by I_R. The actually observed spatial intensity distribution will be a weighted superposition of these two

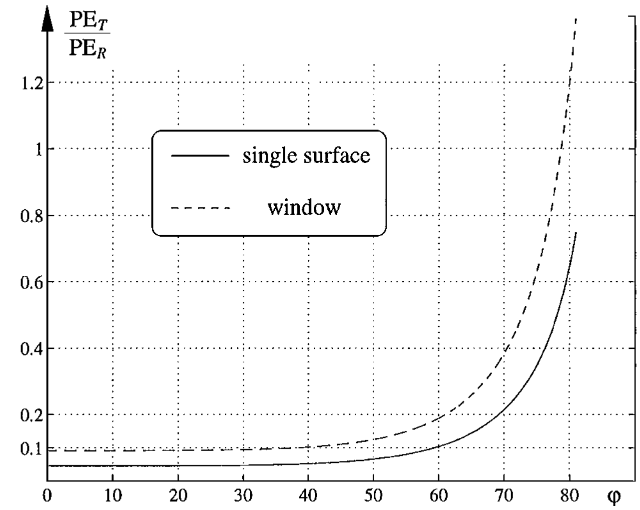

Fig. 1. Ratios of the polarizing effects in a single air–glass interface and in a glass window.

intensities. Let $\theta_\perp$ be the orientation of the polarization analyzer for the best transmission of the component perpendicular to the plane of incidence. Assuming initially unpolarized light and a general orientation of the analyzer α, the observed intensity is given by

$$f(\alpha) = \left(\frac{f_\perp + f_\parallel}{2}\right) + \left(\frac{f_\perp + f_\parallel}{2}\right)\cos[2(\alpha - \theta_\perp)], \qquad (2)$$

where

$$f_\perp = f(\theta_\perp) = (I_R\tilde{R}_\perp/2 + I_T\tilde{T}_\perp/2), \qquad (3)$$

$$f_\parallel = f(\theta_\perp + 90°) = (I_R\tilde{R}_\parallel/2 + I_T\tilde{T}_\parallel/2). \qquad (4)$$

Suppose now that we have an estimate of the geometry of the setup, that is, the plane of incidence (hence $\theta_\perp$) and AOI φ. Then

$$\hat{I}_T(\varphi) = \left[\frac{2\tilde{R}_\perp(\varphi)}{\tilde{R}_\perp(\varphi) - \tilde{R}_\parallel(\varphi)}\right]f_\parallel - \left[\frac{2\tilde{R}_\parallel(\varphi)}{\tilde{R}_\perp(\varphi) - \tilde{R}_\parallel(\varphi)}\right]f_\perp, \qquad (5)$$

$$\hat{I}_R(\varphi) = \left[\frac{2 - 2\tilde{R}_\parallel(\varphi)}{\tilde{R}_\perp(\varphi) - \tilde{R}_\parallel(\varphi)}\right]f_\perp - \left[\frac{2 - 2\tilde{R}_\perp(\varphi)}{\tilde{R}_\perp(\varphi) - \tilde{R}_\parallel(\varphi)}\right]f_\parallel. \qquad (6)$$

As expected, the reconstructions become unstable as $(\tilde{R}_\perp - \tilde{R}_\parallel) \to 0$, that is, at very low or high AOI. Inserting Eqs. (3) and (4), which are based on the true AOI, φ_{true}, into Eqs. (5) and (6), with an assumed φ, we obtain that

$$\hat{I}_T(\varphi) = (1 - \rho)I_T + \rho I_R, \qquad \hat{I}_R(\varphi) = (1 - \tau)I_R + \tau I_T, \qquad (7)$$

where

$$\rho(\varphi_{\text{true}}, \varphi) = \frac{\tilde{R}_\perp(\varphi)\tilde{R}_\parallel(\varphi_{\text{true}}) - \tilde{R}_\perp(\varphi_{\text{true}})\tilde{R}_\parallel(\varphi)}{\tilde{R}_\perp(\varphi) - \tilde{R}_\parallel(\varphi)}, \qquad (8)$$

$$\tau(\varphi_{\text{true}}, \varphi) = \frac{\tilde{T}_\perp(\varphi)\tilde{T}_\parallel(\varphi_{\text{true}}) - \tilde{T}_\perp(\varphi_{\text{true}})\tilde{T}_\parallel(\varphi)}{\tilde{T}_\perp(\varphi) - \tilde{T}_\parallel(\varphi)}. \qquad (9)$$

To estimate the AOI requires an assumption that is related to multiple points. We assume that the real and the virtual scenes are uncorrelated. This is a reasonable supposition because the two scenes usually originate from unrelated objects. Our approach is thus to search for the zero crossing of the correlation between the estimated images:

$$\hat{\varphi} = \{\varphi\colon \quad \text{Corr}[\hat{I}_T(\varphi), \hat{I}_R(\varphi)] = 0\}. \qquad (10)$$

For any two images $\mathbf{p}$ and $\mathbf{q}$ the cross correlation is $\text{Corr}(\mathbf{p}, \mathbf{q}) = \text{Cov}(\mathbf{p}, \mathbf{q})/[\text{Var}(\mathbf{p})\text{Var}(\mathbf{q})]^{1/2}$, where Var denotes the (spatial) variance. The covariance is estimated in the N-pixel images as $\text{Cov}(\mathbf{p}, \mathbf{q}) \simeq \langle \mathbf{p} - \mu_p, \mathbf{q} - \mu_q\rangle/N$, where μ_p is the mean of $\mathbf{p}$. The zero crossing of the correlation occurs at the zero crossing of the cross covariance. Assuming that there is no correlation between I_R and I_T,

$$\text{Cov}(\hat{I}_T, \hat{I}_R) = \tau(1 - \rho)\text{Var}(I_T) + \rho(1 - \tau)\text{Var}(I_R). \qquad (11)$$

This covariance vanishes for $\varphi = \varphi_{\text{true}}$, where ρ, $\tau = 0$ [see Eqs. (8) and (9)]. For all other cases, $[\tau(1 - \rho)]$ has no zero, and we may write Eq. (11) as

$$\text{Cov}(\hat{I}_T, \hat{I}_R) = \tau(1 - \rho)\text{Var}(I_R)\left[\frac{\text{Var}(I_T)}{\text{Var}(I_R)} - \eta\right], \qquad (12)$$

where $\eta(\varphi_{\text{true}}, \varphi) = -[\rho(1 - \tau)]/[\tau(1 - \rho)]$. If φ is allowed to take values arbitrarily close to 90°, η can take any positive value. Thus, if φ is not bounded by some practical limit, a zero of the cross covariance [Eq. (12)] appears at an additional assumed AOI beside the correct one (Fig. 2).

We imaged a scene composed of several objects at a distance of ≈3.5 m through an upright glass window. The window semireflected another scene. A

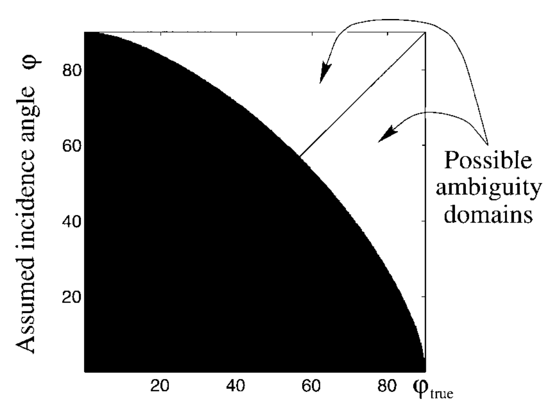

Fig. 2. For each φ_{true} there are domains (white) where a zero of the correlation exists at a wrongly assumed angle φ (beside the correct one).

Fig. 3. Top left, $f_\perp$. Top right, the reflection is weaker in $f_\parallel$, but the image is still unclear. Middle row, the reconstructed virtual (left) and real (right) scenes, based on the automatic detection of the AOI. Bottom right, the real object imaged without the interfering glass window. Bottom left, the virtual object photographed by a technique that removes the objects behind the window.

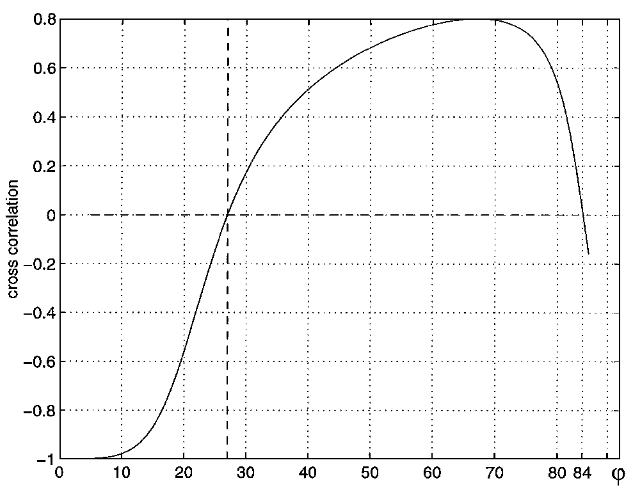

Fig. 4. At the estimated incidence angle of 27° the reconstructions are decorrelated.

linear polarizer was rotated in front of the camera between consecutive image acquisitions. The plane of incidence was horizontal; thus it was easy to obtain $\theta_\perp$ and take the images[9] of $f_\perp$ and $f_\parallel$, which are shown in the top row of Fig. 3. These images are not sensitive to small errors in the estimation of $\theta_\perp$ because, from Eq. (2),

$$\left.\frac{\partial f}{\partial \theta_\perp}\right|_{\alpha=\theta_\perp,\,\theta_\perp+90^\circ} = 0\,. \tag{13}$$

As can be seen from $f_\parallel$, although the polarizer produces some attenuation of the reflected scene, a significant disturbance that is due to this scene remains because $\varphi_{\text{true}} = 27.5^\circ \pm 3^\circ$ is far from the Brewster angle (56°).

The AOI φ to be estimated was assumed to lie between 5° and 85°. At the assumed AOI of $\varphi = 27^\circ$ the estimated layers are decorrelated (Fig. 4), in excellent agreement with the angle used in the physical experimental setup. A second zero crossing of the correlation coefficient exists at 84°, which is in agreement with the theory because for this φ_{true} the threshold for the appearance of a wrong crossing is 80° (see Fig. 2). Using the correctly estimated angle, we applied Eqs. (5) and (6) at each point in the images shown in the top row of Fig. 3. The results, shown in the middle row of Fig. 3, can be compared with the original images shown in the bottom row. Thus, relying on the physical processes involved, we could reconstruct the virtual scenes. It should be noted, however, that at a large AOI an additional solution may exist. The present approach significantly extends the useful range of incidence angles for polarization-based clearing of reflecting disturbances. In addition, the method automatically provides information (the inclination angle) about the clear, invisible medium that lies between the observer and the scene.

In conclusion, note that in a real-life situation several degrading effects exist, which are now under investigation. These effects include noise in the recording system, partial polarization of the incident light, and variation of the AOI across the field of view.

This study was partially supported by the Israeli Ministry of Science. J. Shamir's e-mail address is jsh@ee.technion.ac.il.

References

1. H. Fujikake, K. Takizawa, T. Aida, H. Kikuchi, T. Fujii, and M. Kawakita, Opt. Rev. **5,** 93 (1998).
2. Y. Y. Schechner, N. Kiryati, and R. Basri, in *IEEE International Conference on Computer Vision* (Institute of Electrical and Electronics Engineers, New York), pp. 1061–1066.
3. W. A. Shurcliff and S. S. Ballard, *Polarized Light* (Van Nostrand, Princeton, N.J., 1964), pp. 100–104.
4. N. Ohnishi, K. Kumaki, T. Yamamura, and T. Tanaka, in *Computer Vision-ECCV '96*, R. Buxton and R. Cipolla, eds., Vol. 1065 of Lecture Notes in Computer Science (Springer-Verlag, Berlin, 1996), pp. 636–646.
5. D. Weinshall, Nature **341,** 737 (1989).
6. L. B. Wolff, J. Opt. Soc. Am. A **11,** 2935 (1994).
7. H. Farid and E. H. Adelson, "Separating reflections from images by use of independent-components analysis," J. Opt. Soc. Am. A (to be published).
8. M. Born and E. Wolf, *Principles of Optics*, 5th ed. (Pergamon, Oxford, 1975), pp. 38–45.
9. Link to the raw images through http://www.ee.technion.ac.il/~yoavs/publications.